Research Article

Structural and Chemical Characterization of Silica Spheres before and after Modification by Silanization for Trypsin Immobilization

Eduardo F. Barbosa[1,2,3] and Luciano P. Silva[1,2]

[1]*Embrapa Recursos Genéticos e Biotecnologia, Laboratório de Espectrometria de Massa e Laboratório de Nanobiotecnologia, Parque Estação Biológica Final W5 Norte, 70770-917 Brasília, DF, Brazil*
[2]*Universidade de Brasília, Instituto de Ciências Biológicas, Campus Universitário Darcy Ribeiro, 79910-900 Brasília, DF, Brazil*
[3]*Universidade Federal do Oeste da Bahia, Centro das Ciências Biológicas e da Saúde, Campus Edgar Santos, 47808-021 Barreiras, BA, Brazil*

Correspondence should be addressed to Eduardo F. Barbosa; barbosaeduardofernandes@gmail.com
and Luciano P. Silva; luciano.paulino@embrapa.br

In the last decades, silica particles of a variety of sizes and shapes have been characterized and chemically modified for several applications, from chromatographic separation to dental supplies. The present study proposes the use of aminopropyl triethoxysilane (APTS) silanized silica particles to immobilize the proteolytic enzyme trypsin for the development of a bioreactor. The major advantage of the process is that it enables the polypeptides hydrolysis interruption simply by removing the silica particles from the reaction bottle. Silanized silica surfaces showed significant morphological changes at micro- and nanoscale level. Chemical characterization showed changes in elemental composition, chemical environment, and thermal degradation. Their application as supports for trypsin immobilization showed high immobilization efficiency at reduced immobilization times, combined with more acidic conditions. Indirect immobilization quantification by reversed-phase ultrafast high performance liquid chromatography proved to be a suitable approach due to its high linearity and sensitivity. Immobilized trypsin activities on nonmodified and silanized silica showed promising features (e.g., selective hydrolysis) for applications in proteins/peptides primary structure elucidation for proteomics. Silanized silica system produced some preferential targeting peptides, probably due to the hydrophobicity of the nanoenvironment conditioned by silanization.

1. Introduction

Proteomics represents a quite remarkable area of scientific research, specifically in protein chemistry, which developed breathtakingly and quickly [1–4]. Proteomics characterization usually requires some step of enzymatic hydrolysis. However, the application of proteolytic enzymes such as trypsin, for instance, represents a critical factor to increase the costs of this emerging field. In this context, enzyme immobilization is an attempt to reduce costs, since it allows the reuse for several cycles, minimize autolysis events, and even may improve the kinetic patterns of the immobilized enzyme considering the microenvironment generated by immobilization process [5, 6].

An inherent challenge for enzyme immobilization refers to the accurate quantification of enzyme immobilization efficiency. Spectrophotometric or colorimetric techniques have generally low precision and reproducibility. A reliable option is the use of ultrafast liquid chromatography (UF-HPLC) as an advantageous tool to indirectly evaluate the immobilization efficiency. This technique has high reproducibility and accuracy in determining proteins, enzymes,

and other biomolecules concentration because it allows a separate absorption analysis in ultraviolet region after fractionating the molecules in a chromatographic column.

In this study, bovine pancreatic trypsin was immobilized by adsorption on the surface of nonmodified silica spheres (control) and silica spheres modified by silanization with aminopropyl triethoxysilane (APTS). Experimental design was based in the central composite design (CCD) for optimization of immobilization conditions. Scanning electron microscopy (SEM) and atomic force microscopy (AFM) were used for nano/microstructural and nanomechanical characterization. Control and silanized silica spheres were chemically characterized by Fourier transform infrared spectroscopy (FTIR), energy dispersive spectroscopy (EDS), and thermogravimetric/differential analysis (TGA/DTA). Indirect enzyme immobilization quantification was performed by UF-HPLC. Bovine serum albumin (BSA) was used as protein model for hydrolysis by immobilized trypsin and major peptide fragments generated by the process were chromatographically separated, collected, and identified by matrix assisted laser desorption/ionization time-of-flight mass spectrometry (MALDI-TOF MS). The hypotheses tested in this study were as follows: (i) can silica chemically modified with APTS alters nanoroughness and nanomechanics of sphere surface? (ii) Could the surface modification affect or even modulate trypsin immobilization features and its activity?

2. Material and Methods

2.1. Silanization of Silica Particles. Silica particles with average diameter around 1–4 mm were obtained (Silica gel, Reagen). For silica silanization, dry silica particles (8 g) were treated with APTS (5.2 g) dissolved in toluene (115 mL) at 80 rpm constant stirring for 4 h at room temperature. Treated silica was filtered under vacuum and washed three times with excess toluene. After filtration, the material was dried at 150°C for 4 h and then stored in a sealed plastic bottle protected from light.

2.2. Enzyme Immobilization. Bovine pancreatic trypsin (EC 3.4.21.4) manufactured by Sigma (type I, double-crystallized, Switzerland) was used in the immobilization and activity verification assays. Silanized silica spheres were incubated with a $2 \mu mol \times L^{-1}$ trypsin solution maintaining 0.25 g support $\times 5 mL^{-1}$ enzyme solution ratio. Reaction temperature was kept at 4°C. pH values combinations (ranging from 5.6 to 9.2, by using sodium acetate buffer, sodium phosphate, Tris-HCl, and sodium bicarbonate $0.1 mol \times L^{-1}$) and reaction time (ranging from 10 to 110 min) were determined by central composite design (CCD). Immobilization efficiency was determined indirectly (nonimmobilized fraction) by UF-HPLC.

2.3. Experimental Design. CCD is a two-level classical factorial planning ($2k$), plus some experimental points (star points) for coefficients estimation of a second-order surface. In the present study, CCD was performed using Statistica 8.0 software. CCD was used for simultaneous verification of pH and immobilization time influence (Table 1). Adjustments

TABLE 1: Experimental, coded, and uncoded planning matrix for the central compound design (CCD) for pH and immobilization time.

Experiment number	pH	Time (min)
1	6.0 (−1)	30 (−1)
2	6.0 (−1)	90 (+1)
3	8.6 (+1)	30 (−1)
4	8.6 (+1)	90 (+1)
5	5.8 (−1.26)	60 (0)
6	9.24 (+1.26)	60 (0)
7	7.6 (0)	21.98 (−1.26)
8	7.6 (0)	98.01 (+1.26)
9 (C)	7.6 (0)	60 (0)
10 (C)	7.6 (0)	60 (0)
11 (C)	7.6 (0)	60 (0)
12 (C)	7.6 (0)	60 (0)
13 (C)	7.6 (0)	60 (0)

were model 2xx (2) cube + star; number of factors equal to 2; number of blocks equal to 1; number of runs equal to 10; central number (cn) equal to 4; (Ns) equal to 4 and number zero (n0) equal to 2. Turnover value (α) was 1.4142 and 1.0781 orthogonality.

2.4. Atomic Force Microscopy. Small fragments of non-modified (control) and modified (silanized) silica spheres were fixed on a metallic sample holder using a double-sided adhesive tape. Spheres surface were analyzed using a commercial AFM instrument SPM-9600 (Shimadzu, Kyoto, Japan) operating in contact mode using a typical V-shaped $200 \mu m$ length cantilever integrated with pyramidal silicon nitride tip with 20 nm of curvature radius, spring constant of about $0.15 N \cdot m^{-1}$, and resonance frequency of approximately 24 kHz. The scanner used has a maximum travel of $125 \mu m$ in XY-directions and $7 \mu m$ in Z-direction. Images were obtained in ambient air at 23°C and 30–40% relative humidity. Scanned areas were perfect squares measuring $2.5 \mu m \times 2.5 \mu m$ with a scan rate of 1 Hz. Trace and retrace procedures were performed in order to confirm that samples were not modified during scanning steps. All AFM images contained 512×512 lines and they were processed using SPM-9600 offline software (Shimadzu, Kyoto, Japan). Image processing consisted in an automatic X-line, Y-line, and plane fit leveling of the images. After image processing, surface analysis procedures were performed and the nanoroughness quantitative parameters arithmetic mean roughness (R_a), maximum height (R_z), 10-point mean roughness (R_{zjis}), root-mean-square roughness (R_q), average height (R_p), and average depth (R_v) were calculated from images. One-way ANOVA followed by Tukey's post hoc comparison tests was performed using the Origin Pro 8 software (OriginLab, Northampton, MA).

2.5. Force Spectroscopy. Surface interaction properties were measured by force-distance curves in order to analyze the sphere fragments surface of control and silanized silica using

the same previously described commercial AFM instrument and cantilever-tip set-up. At least 100 force curves were measured for each sample. The acquisition conditions were rate of 1 Hz, amplitude of 20 V, and operating point of 3 V. Force curve parameters were calculated using Scanning Probe Image Processor (SPIP) software (version 5.0, Image Metrology, Lyngby, Denmark) set to 23°C, 0.15 N·m^{-1} spring constant, cone indentation (Sneddon), five fitting points, and approach curve as baseline correction. Statistical analysis (ANOVA and Tukey's test) was performed by Origin Pro 8 software.

2.6. Fourier Transform Infrared Spectroscopy (FTIR). Infrared absorption spectra were obtained using a Fourier transform infrared spectrometer-4100 (Jasco, UK), with wavenumbers ranging from 500 to 4,000 cm^{-1}. Samples analyses were performed in solid state, and a small fragment of each silica sphere was powdered and deposited in the attenuated total reflectance (ATR) system for subsequent acquisition. The reported spectra were averages of 32 scans.

2.7. Scanning Electron Microscopy (SEM) and Energy Dispersive X-Ray Spectroscopy (EDS). SEM and EDS analyses were performed using a JSM 700-1F instrument (JEOL, Japan). A small fragment of each silica sample was fixed on a metallic holder (Cu and Zn) using a double-sided adhesive tape. Thus, samples were sputter coated with gold (Au) using a Balzers SCD 050 (Baltec, Austria) at 21°C, in about 2.6×10^{-7} Pa for 180 s. After coating with Au, the images were obtained applying 15 kV, followed by EDS spectra acquisition with the same voltage and setting live time of 30 s.

2.8. Thermogravimetric Analysis (TGA). The samples were characterized by TG/DTG and DTA using a thermogravimetric and differential thermal analysis DTG-60H/Shimadzu (Japan) simultaneous analyzer using about 5 mg of platinum crucible sample at a 10°C × min^{-1} heating rate ranging from 25 to 750°C, under inert atmosphere (30 mL × min^{-1}). Maximum decomposition rates temperatures (Td) were obtained from DTG curves.

2.9. Quantification of Immobilization Efficiency by UF-HPLC. Chromatographic separation of trypsin solution 52 μmol × L^{-1} (100%) and some fractional dilutions (related to 90%; 80%; 70%; 60%; 50%; 40%; 30%; 20%; 10%; 5%; and 2.5% of initial concentration) was performed. UF-HPLC equipment was a Shimadzu (model LC-20AD, Japan), with a Shim-pack XRODS 2.0 × 50 mm. Apolar solvent concentration gradient (solvent B, acetonitrile in 0.1% TFA) was 5% to 3 min (isocratic condition), following the linear increase in two ranges: up to 65% at 18 min and from 65% to 95% at 20 min, remaining in this condition until 23 min. Solvent A refers to TFA 0.1%. Flow rate was 0.5 mL × min^{-1}. Each chromatographic separation had an injection volume of 50 μL, and the absorbance was monitored at 216 and 280 nm (UV/Vis SPD-20A Detector, Shimadzu, Japan). Areas under trypsin peaks were calculated using the LC Solution software (Shimadzu), and each absolute under the curve area was used in the standard curves elaboration. Trypsin fraction had its identity confirmed by MALDI-TOF MS using an UltraFlex III MALDI-TOF mass spectrometer (Bruker Daltonics, Germany).

2.10. Immobilized Trypsin Activity Assay. One mg × mL^{-1} BSA (at substrate/immobilized enzyme 1 : 10 proportion) was digested with trypsin immobilized in control and silanized silica spheres buffered in 100 mmol ammonium bicarbonate (1 mL), pH 8.0, for 24 h. The peptides obtained through enzymatic digestion were chromatographically fractioned by UF-HPLC set at the same conditions previously described for immobilization efficiency quantification. The fractions were analyzed by MALDI-TOF/TOF MS. All the MS analyses were performed in a Bruker Daltonics UltraFlex III. Samples were mixed with a saturated alpha-cyano-4-hydroxycinnamic acid solution (1 : 3) and applied (0.5 μL) in duplicate on an MTP AnchorChip var/384 type plate. Molecular masses ranged from m/z 600 to 2500 using the positive reflected mode. Fragmentations for manual de novo peptide sequencing were performed by MALDI-TOF/TOF MS using the LIFT® method. Sequencing was manually performed by using the FlexAnalysis 3.0 software.

3. Results and Discussion

Figure 1 shows images of control (Figure 1(a)) and silanized silica surfaces (Figure 1(b)) obtained by SEM. At these magnifications, it is possible to visualize clearly that the silanization process drastically alters topographical features of silica particles surfaces. Images obtained through AFM analysis confirm that morphological changes caused by silanization process also affect nanoscale features (Figures 1(c) and 1(d)). Roughness quantitative results (R_a, R_z, R_{zjis}, R_q, R_p, and R_v) calculated from AFM images are shown in Figure 1(e). Roughness results regarding silanized silica were all higher than those observed for control, and all parameters showed statistically significant differences ($p < 0.05$). R_a, R_q, R_z, and R_v values were approximately 2-fold higher in modified silica; R_{zjis} was 6.5-fold higher; and R_p was about 7-fold higher. Qualitative examinations of microscopic images (Figures 1(a), 1(b), 1(c), and 1(d)) could suggest that silanized silica particles had flatter plateaus on their surface when compared to nonsilanized surfaces, which have seemingly larger amount of irregularities. However, considering the nanoscale quantitative approach, it was showed that the silanization process beyond significantly increased all the roughness results, and it also clearly increased heterogeneity considering either these average results or the standard error values increase of each roughness parameter in modified silica.

From the 60s to 90s, one can find in the literature several studies related to silica particles silanization [7–11]. The major applications described for these functionalized materials were related to their use in filling of columns used for liquid and gas chromatographic separation. It occurs because of their typical hydrophobicity, roughness, and surface area properties [7–16]. More recently, another field in which silanized silica materials have received special
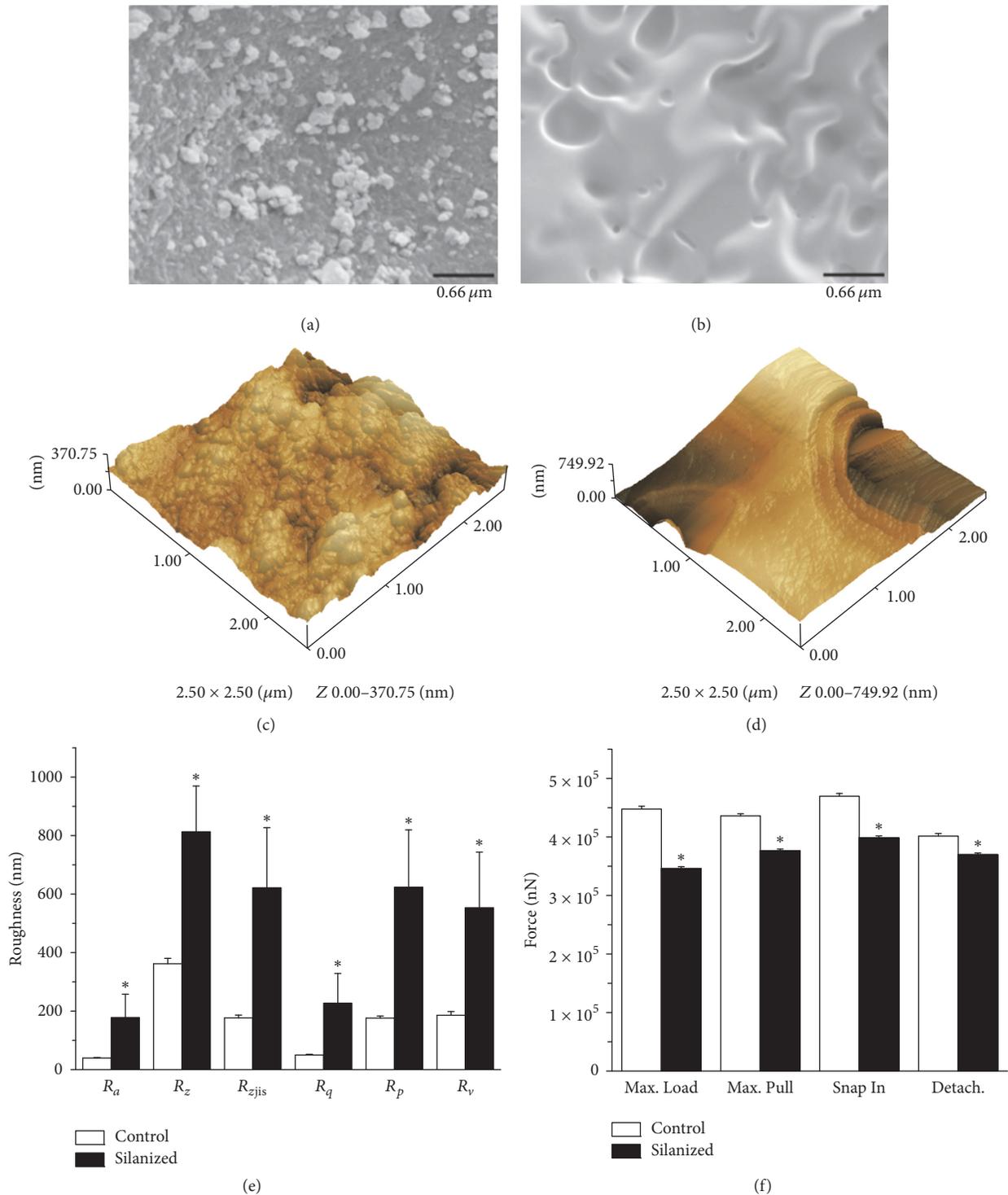
FIGURE 1: Topographical images obtained by scanning electron microscopy (SEM) of control (a) and silanized silica surfaces (b) and atomic force microscopy (AFM) analysis (operating in contact mode) of control (c) and silanized silica (d). Graphical representation of roughness parameters results (R_a, R_z, R_{zjis}, R_q, R_p, and R_v) related to control and silanized silica obtained by AFM (e). Force spectroscopy results obtained by force versus displacement curves analyses performed in an atomic force microscope operating in contact mode (f). $*$ indicates statistically significant difference ($p < 0.05$).

attention is their use as dental materials [17–20]. Tsai et al. [21] made up a self-assembled film by deposition of silanized silica particles to obtain a surface with hydrophobic properties. They demonstrated that silanization significantly increased the surface roughness of the films (about 1.9-fold). Rinastiti et al. [19] obtained similar results when investigating dental resin composites containing silanized silica particles. D'Acunzi et al. [22] showed the use of silanized silica particles as a way to obtain superhydrophobic surfaces with the roughness adjusted by the drying process. Finally, Han et al. [20] compared three resins for dental repair, and those obtained from silanized silica had significantly higher surface roughness.

Figure 1(f) shows nanomechanical results obtained from force-distance curves of control and silanized silica surfaces. In contrast to quantitative roughness results, all force spectroscopy parameters were significantly decreased ($p < 0.05$) on modified surfaces when compared to the control. This implies that modified silica surface showed lower hardness (considering Max Load force parameter, which was 29% lower than control), lower adhesion tendencies (considering Max Pull force and Detachment force parameters, which were 10–15% lower than control), and decreased attractive forces (considering snap in force parameter, which was 10% lower comparing to the control). Considering the medical/odontological applications of silanized composites, in general, higher values of shear force obtained after silanization have been reported [23–25].

Figure 2(a) shows EDS results concerning the relative elemental composition of control and silanized silica. Silicon level remains almost unchanged, while carbon composition of silanized silica particles showed remarkable increase, due the attachment of APTS propyl groups to the surface. Figure 2(b) shows the chemical environment of control and silanized silica surfaces obtained by FTIR analysis. In a first overview, it is clear that silanized silica has transmittance bands with higher intensities when compared to control. Bands between 1100 and 960 cm^{-1} relate to silica and can be found in both spectra (Si-O-Si and Si-O-H stretching, resp.). Transmittance bands at about 3455, 3010, 2969, and 2940 cm^{-1} appear only in silanized silica sample, resulting from APTS chemical modification process, similar to those assignments from Ramos et al. [26]. Water adsorption presence was evidenced by 3455 cm^{-1} band, especially in silanized silica, together with amino group bands (N-H bound, 1560 cm^{-1}). Figure 2(c) shows the results obtained by thermogravimetric analysis for control and silanized silica. There were two decomposition steps when temperature ramped from 25 to 850°C, and both samples showed a similar weight loss considering the first weight loss stage (Table 2). Table 2 shows also the heat losses related to control and silanized silica particles. It indicated that, in the second stage, the exothermic peak of silanized silica showed a differential event, which relates directly to silanization process. Kursunlu et al. [27] described similar results obtained by EDS, FTIR, and TGA characterizations of silanized and nonmodified silica particles. Prado et al. [28] and Sales et al. [29] described similar TGA results.

Table 2: Thermogravimetric/differential analysis (TGA/DTA) for control and silanized silica thermal decomposition.

Sample	Decomposition temperature T_d (°C)	Weight loss (%)
1st stage		
Control	63.35	19.7
Silanized	58.21	21.3
Heat loss (J/g)		
1st stage		
Control	−897.37	
Silanized	−930.25	
2nd stage		
Control		
Silanized	37.86	
3rd stage		
Control	−125.05	
Silanized	−117.14	
4th stage		
Control	−29.43	
Silanized		

The quantification of the immobilization efficiency and determination of enzyme concentration in solutions represent uncertainty factors, since the traditional methods are usually colorimetric and associated with high levels of experimental error. Accordingly, we used UF-HPLC due to its high accuracy and reproducibility. Then, a standard curve was obtained by using enzyme concentrations ranging from 52 μM (100%) to 1.3 μM (2.5%) (Figure 3(a)). The fraction containing the enzyme was measured by integration of the areas under the peaks matching the trypsin. A high linearity between integrated areas and relative concentrations was observed ($R^2 = 0.9974$), as shown in Figure 3(b).

The next step was the trypsin immobilization assays in control and silanized silica particles. Experimental design was a CCD model, which enabled the simultaneous verification of the pH and immobilization time over immobilization efficiency, as shown in Figures 4(a) and 4(b). Both systems showed high trypsin immobilization efficiency (between 80 and 98%) at the concentration tested. Whereas control (Figure 4(a)) showed a broader range of pH values with higher immobilization efficiency, silanized particles (Figure 4(b)) showed higher trypsin immobilization at lower pH values associated with decreased immobilization times. This effect probably occurs due to APTS presence on silica surface, creating a more hydrophobic environment which could have destabilized the immobilization process at higher pH conditions. Díaz and Balkus Jr. [30] immobilized trypsin and other proteins in mesoporous silica by physical adsorption and obtained similar results. They concluded that immobilization was pH dependent, being favored by acidic conditions. They also modified silica by silanization process but performed it after trypsin immobilization process, in order to increase enzyme trapping and reduce leaching losses.

(a)

(b)

(c)
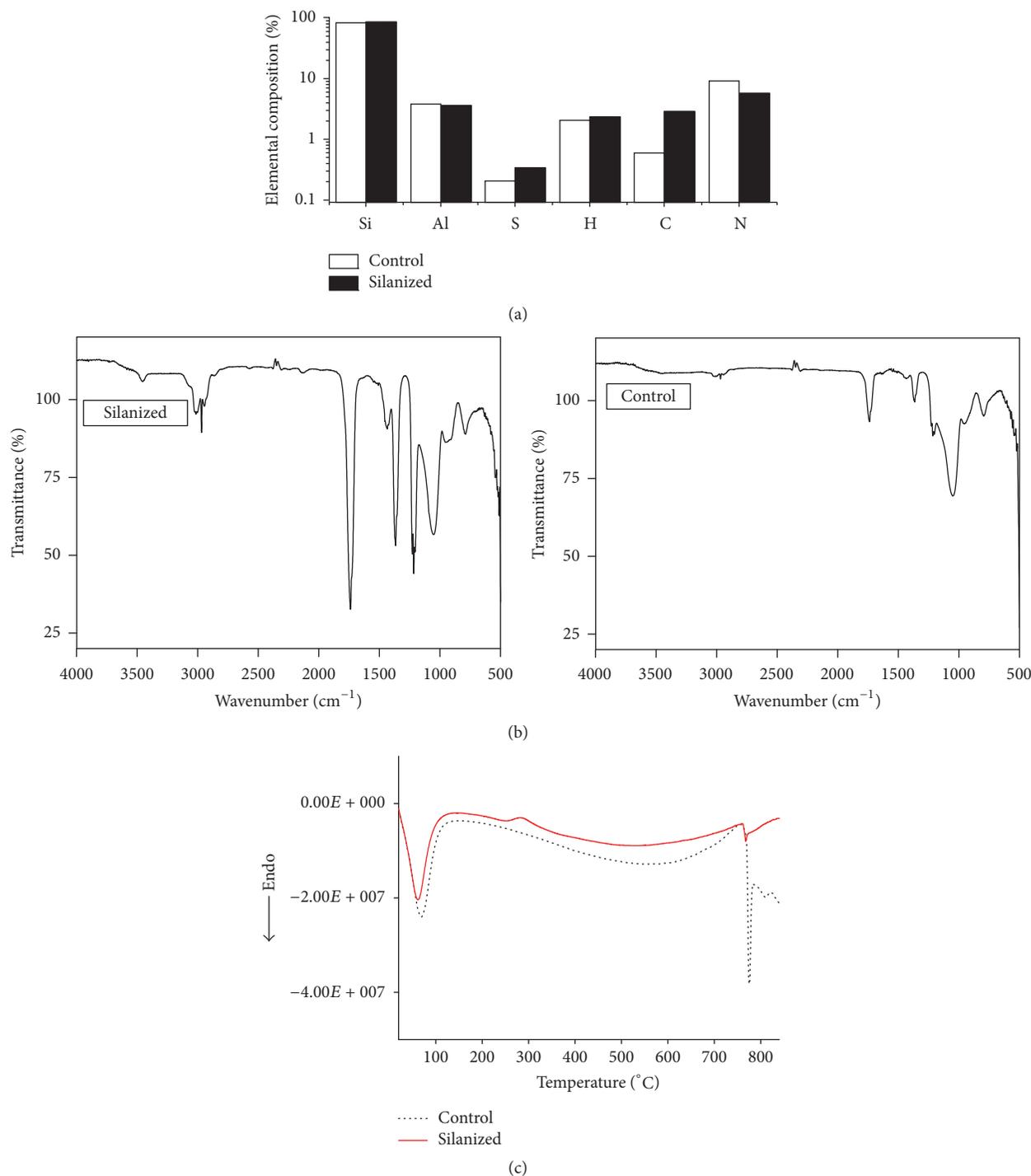
Figure 2: Energy dispersive spectroscopy (EDS) of control and silanized silica surfaces, representing the atoms percentage in each material (a). Fourier transform infrared spectroscopic analyses (FTIR) of control and silanized silica surfaces, using an attenuated total reflectance (ATR) adapter (b). Thermogravimetric analysis (TGA) samples of control and silanized silica (c). Temperature variation ranged between 25 and 850°C.

In the present study, systems containing immobilized trypsin were used for BSA hydrolysis ($1\,mg \times mL^{-1}$). Hydrolysis products were fractioned by UF-HPLC (Figure 5(a)) and each fraction was analyzed by MALDI-TOF MS. Mass spectra related to BSA hydrolysis carried out by immobilized trypsin in control in comparison to silanized silica particles resulted in subtly different molecular mass profiles. Trypsin immobilized in control silica particles produced some ions that were not observed in the hydrolysis performed by immobilized trypsin silanized silica. Figure 5(b) represents

(a)

(b)
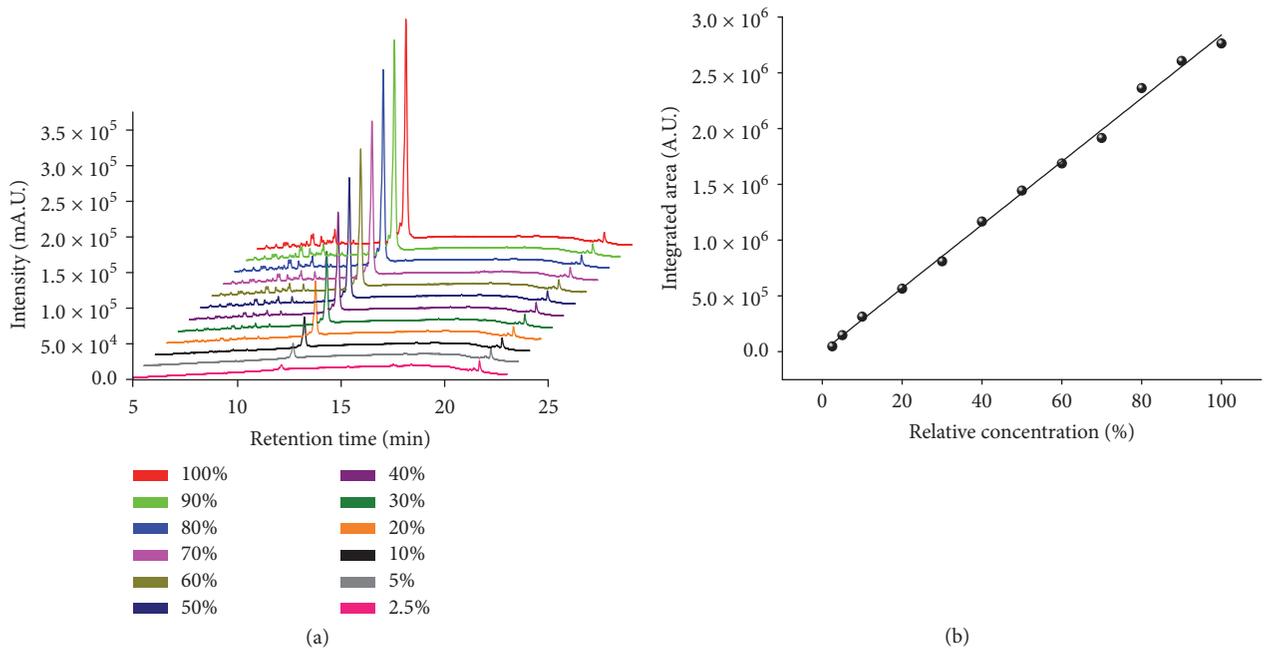
FIGURE 3: Chromatographic separation of trypsin solutions obtained by ultrafast high performance liquid chromatography (UF-HPLC) (a). Trypsin solution concentrations ranged from 52 μM (100%) to 1.3 μM (2.5%), as shown in the color scale. Acetonitrile concentration gradient linearly varied from 5 to 65% in 15 min. Standard curve obtained by integrating the area under the peaks relating to the trypsin corresponding fraction (b).

(a)

(b)
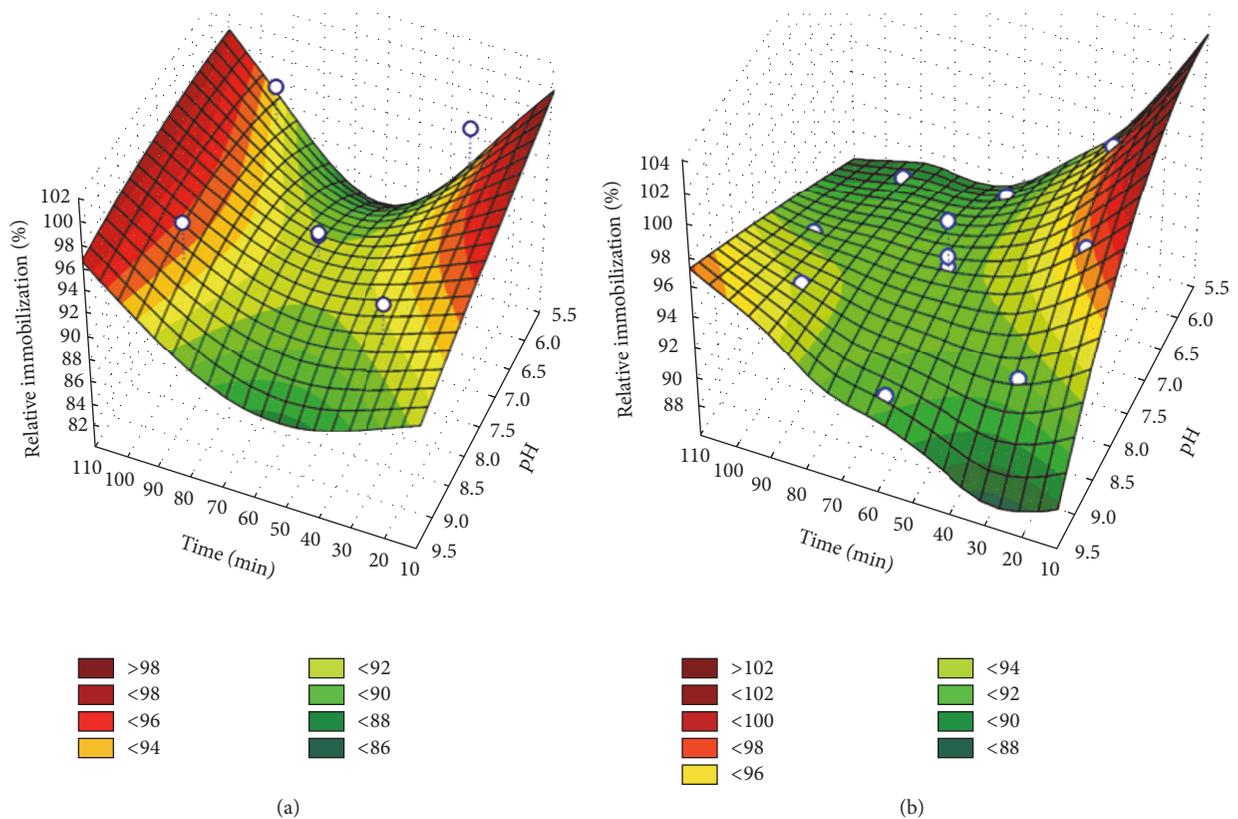
FIGURE 4: Surface response graph regarding the trypsin immobilization efficiency on silica control (a) and silanized (b). "x-axis" represents the pH values, "y-axis" represents the immobilization reaction time, and "z-axis" represents the immobilization efficiency. White dots indicate the tested experimental points.

(a)

(b)

(c)
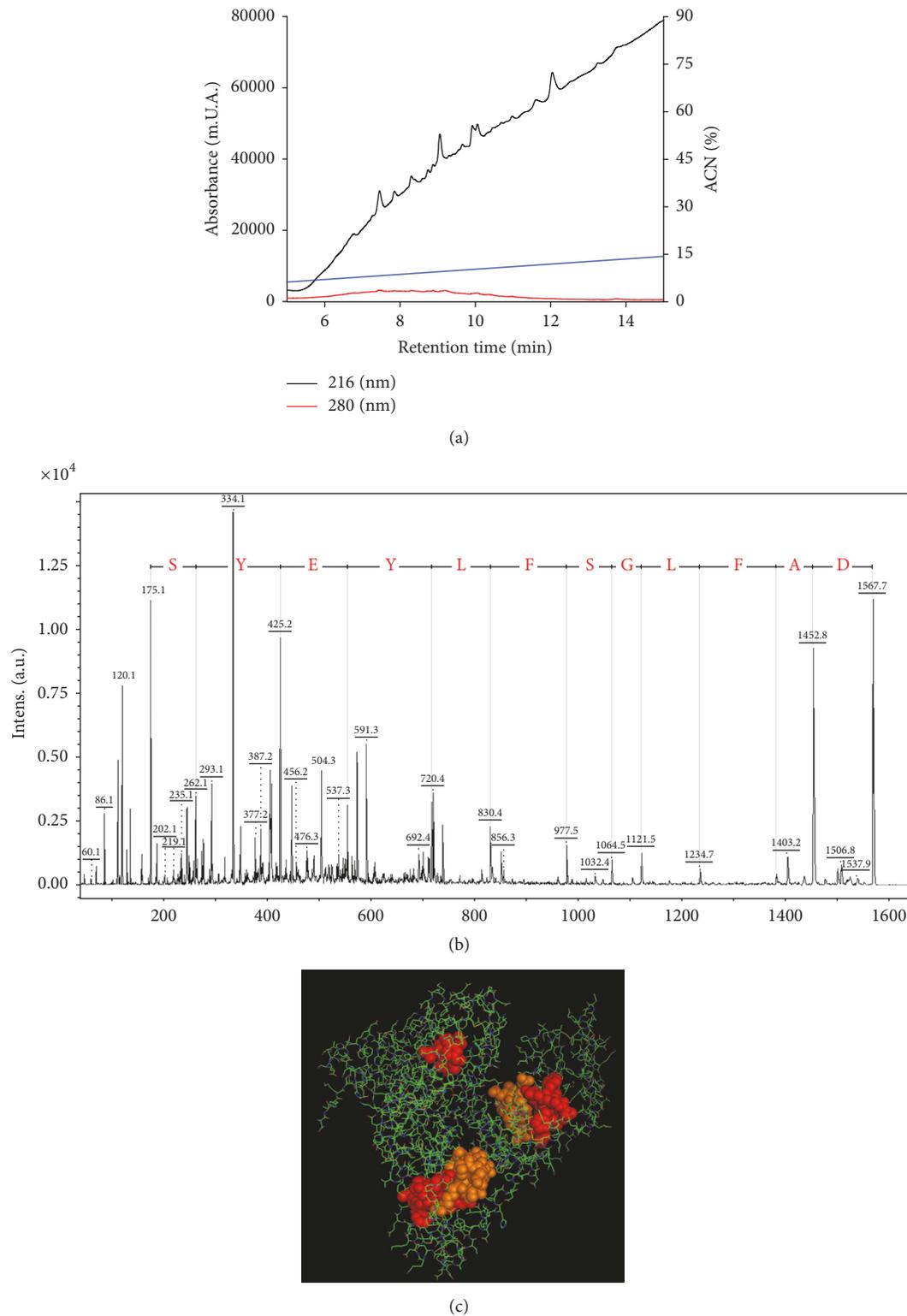
FIGURE 5: Chromatographic separation of bovine serum albumin samples hydrolyzed by trypsin immobilized on silanized silica by ultrafast liquid chromatography (a). Sequencing of $[M + H]^+ = 1567.7$ Da molecular component obtained by the bovine serum albumin hydrolysis using trypsin immobilized in a silanized silica. "y" series ions are shown in the reported sequence (b). Three-dimensional representation of the monomeric bovine serum albumin molecule, highlighting the regions in the molecule that were preferentially cleaved by trypsin immobilized on silanized silica (c). PDB ID code was used: 1E7I and PyMOL molecular graphical tool for image production.

one of the peptides De novo sequenced which were obtained after enzymatic hydrolysis. Figure 5(c) shows the major BSA peptide fragments hydrolyzed by trypsin immobilized on silanized silica particles. It indicates some preferential cleavage activity by specific BSA motifs, which may be a result of the changes in hydrophobicity of the silica surface caused by APTS modification. Wang et al. [31] immobilized trypsin onto a glass coverslip composing a microfluidic device integrated to a mass spectrometer and obtained a similar molecular masses profile when compared to control silica. This fact reinforces a possible preferential pattern of cleavage for trypsin immobilized on modified silica, possibly because of the more hydrophobic environment created by silanized surface.

4. Conclusion

Silica chemical modification by APTS resulted in significant morphological changes in silica spheres surface. Chemical characterization showed changes in elemental composition, chemical environment, and differential thermal degradation for silanized silica particles surface. Such surfaces were used as supports for trypsin immobilization and greater efficiency was observed in reduced immobilization times, combined with more acidic conditions. Indirect immobilization quantification by UF-HPLC proved to be a reliable technique because of high linearity and sensitivity obtained. Immobilized trypsin activities on control and silanized silica surfaces showed promising features for applications in proteins/peptides primary structure elucidation, and silanized silica system produced some preferential targeting motifs concerning the generated peptides, probably due to the more hydrophobicity microenvironment conditioned by silanization.

Conflicts of Interest

The authors declare that they have no conflicts of interest.

Acknowledgments

References

[1] R. Aebersold and M. Mann, "Mass spectrometry-based proteomics," *Nature*, vol. 422, no. 6928, pp. 198–207, 2003.

[2] Y. Ho, A. Gruhler, A. Heilbut et al., "Systematic identification of protein complexes in Saccharomyces cerevisiae by mass spectrometry," *Nature*, vol. 415, pp. 180–183, 2002.

[3] G. Renella, O. Ogunseitan, L. Giagnoni, and M. Arenella, "Environmental proteomics: a long march in the pedosphere," *Soil Biology and Biochemistry*, vol. 69, pp. 34–37, 2014.

[4] M. Larance and A. I. Lamond, "Multidimensional proteomics for cell biology," *Nature Reviews Molecular Cell Biology*, vol. 16, no. 5, pp. 269–280, 2015.

[5] L. L. A. Purcena, S. S. Caramori, S. Mitidieri, and K. F. Fernandes, "The immobilization of trypsin onto polyaniline for protein digestion," *Materials Science and Engineering C*, vol. 29, no. 4, pp. 1077–1081, 2009.

[6] J. N. Talbert and J. M. Goddard, "Enzymes on material surfaces," *Colloids and Surfaces B: Biointerfaces*, vol. 93, pp. 8–19, 2012.

[7] L. R. Snyder and J. W. Ward, "The surface structure of porous silicas," *Journal of Physical Chemistry*, vol. 70, no. 12, pp. 3941–3952, 1966.

[8] B. L. Karger and E. Sibley, "Study of chemically bonded supports in gas chromatography," *Analytical Chemistry*, vol. 45, no. 4, pp. 740–748, 1973.

[9] J. L. M. van de Venne, J. P. M. Rindt, G. J. M. M. Coenen, and C. A. M. G. Cramers, "Synthesis of a nonpolar, chemically bonded stationary phase with low residual hydroxyl group content," *Chromatographia*, vol. 13, no. 1, pp. 11–17, 1980.

[10] B. Porsch, "Silica based aminopropyl-bonded phase trimethylsilylated with N-trimethylsilyli midazole," *Journal of Liquid Chromatography*, vol. 14, no. 1, pp. 71–78, 1991.

[11] H. H. Weetall, "Preparation of immobilized proteins covalently coupled through silane coupling agents to inorganic supports," *Applied Biochemistry and Biotechnology*, vol. 41, no. 3, pp. 157–188, 1993.

[12] E. D. Pellizzari, "High-resolution electron capture gas-liquid chromatography," *Journal of Chromatography A*, vol. 92, no. 2, pp. 299–308, 1974.

[13] A. M. Khalil, "Development of surface porosity by trimethylchlorosilane treatment: nitrogen adsorption measurements on aerosil 200 silica," *Surface Technology*, vol. 14, no. 4, pp. 373–382, 1981.

[14] T. M. Chen and G. M. Brauer, "Solvent effects on bonding organo-silane to silica surfaces," *Journal of Dental Research*, vol. 61, no. 12, pp. 1439–1443, 1982.

[15] G. Schomburg, J. Köhler, H. Figge, A. Deege, and U. Bien-Vogelsang, "Immobilization of stationary liquids on silica particles by γ-radiation," *Chromatographia*, vol. 18, no. 5, pp. 265–274, 1984.

[16] J. Pesek and T. Cash, "A chemically bonded liquid crystal as a stationary phase for high performance liquid chromatography. Synthesis on silica via an organochlorosilane pathway," *Chromatographia*, vol. 27, no. 11-12, pp. 559–564, 1989.

[17] H. H. K. Xu, "Dental composite resins containing silica-fused ceramic single-crystalline whiskers with various filler levels," *Journal of Dental Research*, vol. 78, no. 7, pp. 1304–1311, 1999.

[18] H. H. K. Xu, F. C. Eichmiller, J. M. Antonucci, G. E. Schumacher, and L. K. Ives, "Dental resin composites containing ceramic whiskers and precured glass ionomer particles," *Dental Materials*, vol. 16, no. 5, pp. 356–363, 2000.

[19] M. Rinastiti, M. Özcan, W. Siswomihardjo, and H. J. Busscher, "Immediate repair bond strengths of microhybrid, nanohybrid and nanofilled composites after different surface treatments," *Journal of Dentistry*, vol. 38, no. 1, pp. 29–38, 2010.

[20] I.-H. Han, D.-W. Kang, C.-H. Chung, H.-C. Choe, and M.-K. Son, "Effect of various intraoral repair systems on the shear bond strength of composite resin to zirconia," *Journal of Advanced Prosthodontics*, vol. 5, no. 3, pp. 248–255, 2013.

[21] P.-S. Tsai, Y.-M. Yang, and Y.-L. Lee, "Fabrication of hydrophobic surfaces by coupling of Langmuir-Blodgett deposition and a self-assembled monolayer," *Langmuir*, vol. 22, no. 13, pp. 5660–5665, 2006.

[22] M. D'Acunzi, L. Mammen, M. Singh et al., "Superhydrophobic surfaces by hybrid raspberry-like particles," *Faraday Discussions*, vol. 146, pp. 35–48, 2010.

[23] M. Özcan, P. K. Vallittu, M.-C. Huysmans, W. Kalk, and T. Vahlberg, "Bond strength of resin composite to differently conditioned amalgam," *Journal of Materials Science: Materials in Medicine*, vol. 17, no. 1, pp. 7–13, 2006.

[24] M. Rinastiti, M. Özcan, W. Siswomihardjo, and H. J. Busscher, "Effects of surface conditioning on repair bond strengths of non-aged and aged microhybrid, nanohybrid, and nanofilled composite resins," *Clinical Oral Investigations*, vol. 15, no. 5, pp. 625–633, 2011.

[25] B. Stawarczyk, A. Trottmann, C. H. F. Hämmerle, and M. Özcan, "Adhesion of veneering resins to polymethylmethacrylate-based CAD/CAM polymers after various surface conditioning methods," *Acta Odontologica Scandinavica*, vol. 71, no. 5, pp. 1142–1148, 2013.

[26] M. A. Ramos, M. H. Gil, E. Schacht, G. Matthys, W. Mondelaers, and M. M. Figueiredo, "Physical and chemical characterisation of some silicas and silica derivatives," *Powder Technology*, vol. 99, no. 1, pp. 79–85, 1998.

[27] A. N. Kursunlu, E. Guler, H. Dumrul, O. Kocyigit, and I. H. Gubbuk, "Chemical modification of silica gel with synthesized new Schiff base derivatives and sorption studies of cobalt (II) and nickel (II)," *Applied Surface Science*, vol. 255, no. 21, pp. 8798–8803, 2009.

[28] A. G. S. Prado, J. A. A. Sales, and C. Airoldi, "The increased termal stability associated with humic acid anchored onto silica gel," *Journal of Thermal Analysis and Calorimetry*, vol. 70, no. 1, pp. 191–197, 2002.

[29] J. A. A. Sales, F. P. Faria, A. G. S. Prado, and C. Airoldi, "Attachment of 2-aminomethylpyridine molecule onto grafted silica gel surface and its ability in chelating cations," *Polyhedron*, vol. 23, no. 5, pp. 719–725, 2004.

[30] J. F. Díaz and K. J. Balkus Jr., "Enzyme immobilization in MCM-41 molecular sieve," *Journal of Molecular Catalysis B: Enzymatic*, vol. 2, no. 2-3, pp. 115–126, 1996.

[31] C. Wang, R. Oleschuk, F. Ouchen, J. Li, P. Thibault, and D. J. Harrison, "Integration of immobilized trypsin bead beds for protein digestion within a microfluidic chip incorporating capillary electrophoresis separations and an electrospray mass spectrometry interface," *Rapid Communications in Mass Spectrometry*, vol. 14, no. 15, pp. 1377–1383, 2000.

Journal of
Nanotechnology

International Journal of
Corrosion

International Journal of
Polymer Science

Smart Materials
Research

Journal of
Composites

BioMed
Research International

Journal of
Metallurgy

Journal of
Materials
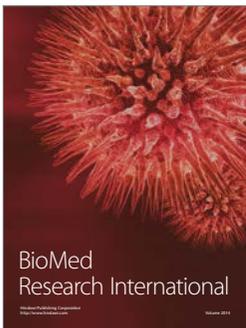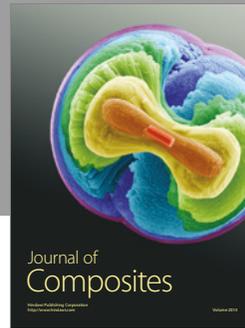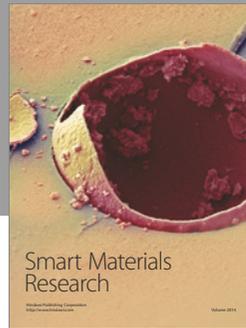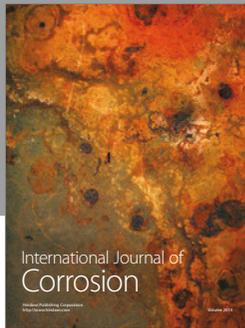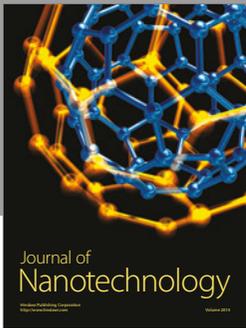
Hindawi

Submit your manuscripts at
https://www.hindawi.com

Journal of
Nanoparticles

Advances in
Materials Science and Engineering

Scientifica

Journal of
Nanomaterials

The Scientific
World Journal

International Journal of
Biomaterials

Journal of
Nanoscience

Journal of
Coatings

Journal of
Crystallography

Journal of
Ceramics

Journal of
Textiles